Cryo-TEMPO

Algorithm Theoretical Basis Document

Polar Ocean

Prepared by	:	S.K. Rose, O. Andersen	22/6/2022
Checked by	:	S. Hendricks	20/7/2022
Approved by	:		

Change Log

Issue	Author	Affected Section	Change	Status
0	S.K. Rose, O. Andersen	All	Document Creation	Complete
1.1	S.K. Rose, O. Andersen	All	Version 1 Content	Complete
2.1	S.K. Rose, O. Andersen	All	Version 1 Revisions	In Review

Acronyms and Abbreviations

AD	Applicable Document	REAPER	Reprocessing of Altimeter Products for ERs
ADT	Absolute Dynamic Topography	RFW	Request for Waiver
ATM	Airborne Topographic Mapper	RMSD	Root mean square difference
AWI	Alfred Wegener Institute	SAR	Synthetic Aperture Radar
C3S	Copernicus Climate Change Service	SARIn	Synthetic Aperture Radar Interferometric
CCI	Climate Change Initiative	SL	Science Lead
CCN	Contract Change Notice	SLA	Sea Level Anomaly
CLS	Collecte Localisation Satellites	SoW	Statement of Work
CNES	Centre National des Etudes Spatiales (French Space Agency)	SS	Shepherd Space
CNR	Consiglio Nazionale delle Ricerche	TCOG	Threshold Centre of Gravity
CPOM	Centre for Polar Observation & Modelling	TDP	Thematic Data Product
CR	Change Request	TFMRA	Threshold First Maximum Retracker Algorithm
CRISTAL	Copernicus Polar Ice and Snow Topography Altimeter	TUG	Thematic User Group
CryoVEx	Cryosat Validation Experiment (field campaigns)	UCL	University College London
DAHITI	Database for Hydrological Time Series of Inland Waters	UCM	User Consultation Meeting
DEM	Digital Elevation Model	WP	Work Package
DTU	Technical University of Denmark	WSH	Water Surface Height
EO	Earth Observation		
ERR	Evolutions Recommendation Report		
ESA	European Space Agency		
FIS	Finnish Ice Service		
FMI	Finnish Meteorological Institute		
FRAPPE	Flexible Radar Altimeter Processor for Performance Evaluation		
FRM4ALT	Fiducial Reference Measurement for Altimetry		
FRD4ALT	Fundamental Data Records for Altimetry		
G-REALM	Global Reservoirs and Lakes Monitor		
IMEDEA	Instituto Mediterráneo de Estudios Avanzados		
IPCC	Intergovernmental Panel on Climate Change		
IRPI	Istituto di Ricerca per la Protezione Idrogeologica		
ISRO	Indian Space Research Organisation		
ITT	Invitation To Tender		
JPL	Jet Propulsion Laboratory		
LEGOS	Laboratoire d'Étude en Géophysique et Océanographie Spatiale		
LRM	Low Resolution Mode		
LU	Lancaster University		
MDT	Mean Dynamic Typography		
MSS	Mean Sea Surface		
MSSL	Mullard Space Science Laboratory (part of UCL)		
NCR	Non Conformance Report		
NERSC	Nansen Environmental and Remote Sensing Center		
OCOG	Offset Centre Of Gravity retracker		
PDS	Payload Data Segment		
PEG	Polar Expert Group		
PM	Project Manager		
PO	Polar Oceans		
PSMSL	Permanent Service for Mean Sea Level		
RA	Radar Altimeter / Altimetry		

Table of Contents

1 INTRODUCTION

1.1 Purpose and Scope

This document comprises the Algorithm Theoretical Basis (ATBD) for the polar ocean algorithm used for the *CryoSat-2 ThEMatic PrOducts* (*Cryo-TEMPO*) study, Ref: ESA AO/1-10244/2-/I-NS. The ATBD has been written by the Polar Ocean Team led by DTU, with contributions from all members of the Cryo-TEMPO consortium, but especially the sea ice team has contributed as the polar ocean algorithm steam from the sea ice algorithm. Lancaster University as the prime contractor is the contact point for all communications regarding this document.

1.2 Document Structure

The document is structured as follows:

- **Section 1 – Introduction**
- **Section 2.1 – Polar Ocean Parameter Definition**
- **Section 2.2 – Overall Polar Ocean Processing Flow**
- **Section 2.4 – Polar Ocean Source Data**
- **Section 2.5 – Polar Ocean Algorithm Descriptions**
- **Section 3 – Assumptions and Known Issues**

1.3 Applicable and Reference Documents

Applicable documents

Reference	Title
AD1	Statement of Work ESA Express Procurement Plus - EXPRO+ CryoSat-2 ThEMatic PrOducts | Cryo-TEMPO, Issue 1, Revision 0, Date of Issue 01/04/2020 [Ref. ESA-EOPG-EOPGMQ-SOW-10].
AD2	Invitation to Tender for CryoSat-2 ThEMatic PrOducts | Cryo-TEMPO REF.: ESA AO/1-10244/2-/I-NS [Ref. SA-IPL-POE-NS-sp-LE-2020-313].
AD3	Draft Contract, CryoSat-2 ThEMatic PrOducts | Cryo-TEMPO, Appendix 2 to ESA AO/1-10244/20/I-NS.

Reference documents

Reference	Title
RD1	Copernicus Polar and Snow Cover Applications User Requirements Workshop, http://www.copernicus.eu/polar-snow-workshop
RD2	PEG-1 Report, User Requirements for a Copernicus Polar Mission, Step 1 Report, Polar Expert Group, Issue: 12th June 2017
RD3	PEG-2 Report, Polar Expert Group, Phase 2 Report on Users Requirements, Issue: 31st July 2017
RD4	CryoSat-2 Product Handbook Baseline D 1.1 C2-LI-ACS-ESL-5319

2 SEA LEVEL ANOMALY AND DYNAMIC OCEAN TOPOGRAPHY

2.1 Parameter Definition

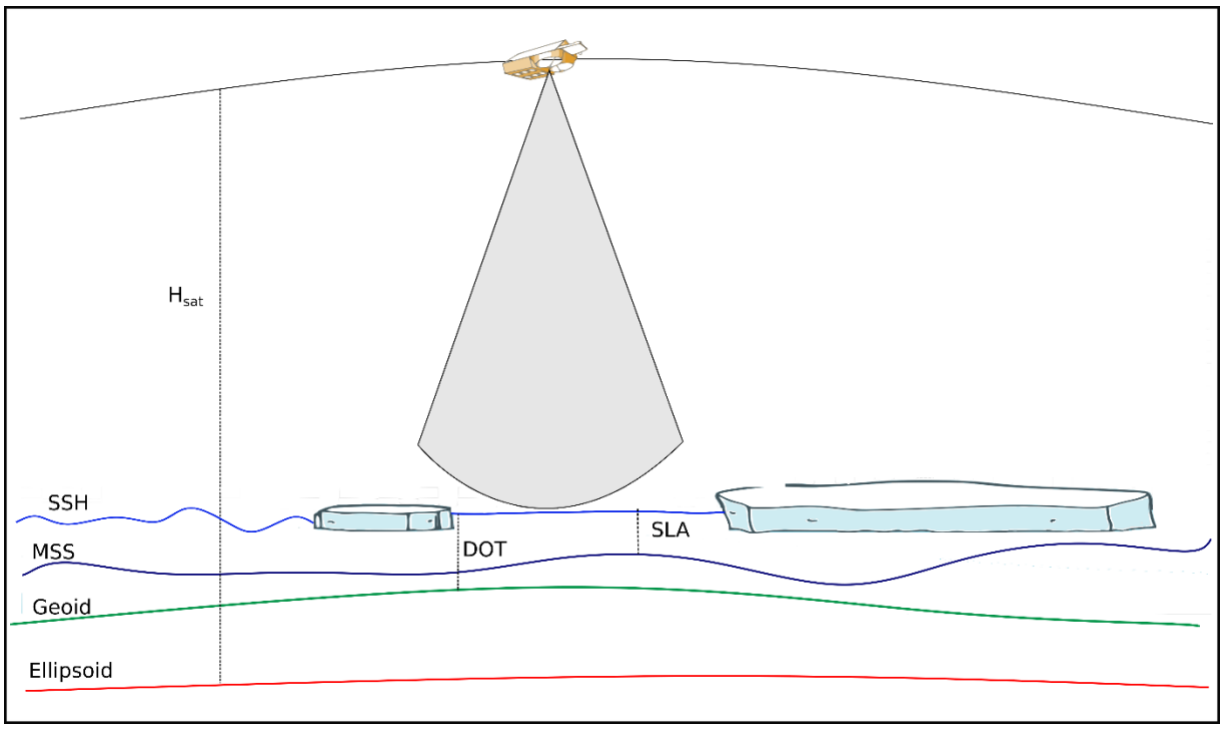

Figure 1: Schematic of sea level anomaly (SLA) and dynamic ocean topography (DOT) retrieval from CryoSat-2 altimeter track data.

The Cryo-TEMPO thematic polar ocean product contains sea level anomaly, the elevation of the sea surface of the polar oceans above a mean sea surface, as well as the dynamic ocean topography above a geoid. A full definition of the two parameters as well as their standardizes names are given in Table 1.

Table 1: Definition of polar ocean variables in the Cryo-TEMPO thematic polar ocean product.

Parameter	**Property**	
Time	*Unit*	UTC
	Standard Name	time
	Definition	UTC time of measurement acquisition
Latitude	*Unit*	Degrees
	Standard Name	lat

	Definition	Latitude of estimated echo location [-90,+90]. Positive latitude is North latitude, negative latitude is South latitude.
Longitude	*Unit*	Degrees
	Standard Name	lon
	Definition	Longitude of estimated echo location [-180,+180]. East longitude relative to Greenwich meridian.
Sea Level Anomaly	*Unit*	Meter (m)
	Standard Name	sea_level_anomaly
	Definition	Sea level anomaly is defined as the height of water above a mean sea surface. In this case the DTU21MSS. The DTU21 MSS has a 20 year mean reference period (1993-2012) using up-to-date multi-mission altimeter measurements. Smoothing has been applied to the measurements, and the measurements are interpolated at sea ice covered locations.
Dynamic Ocean Topography	*Unit*	Meter (m)
	Standard Name	dynamic_ocean_topography
	Definition	Dynamic ocean topography is defined as the height of water above the OCMOG geoid.
Raw sea level anomaly	*Unit*	Meter (m)
	Standard Name	Sea_level_anomaly_raw
	Definition	The raw sea level anomalies. No interpolation, smoothing nor filtering applied.
Filtered Sea Level Anomaly	*Unit*	Meter (m)
	Standard Name	sea_level_anomaly_smooth
	Definition	Smoothed sea level anomaly with a LOWESS filter
Filtered Dynamic Ocean Topography	*Unit*	Meter (m)
	Standard Name	sea_level_anomaly_smooth
	Definition	Smoothed dynamic ocean topography with a LOWESS filter
Uncertainty Sea Level Anomaly	*Unit*	Meter (m)
	Standard Name	uncertainty_sea_level_anomaly
	Definition	Uncertainty of the SLA measurements
Uncertainty Dynamic Ocean Topography	*Unit*	Meter (m)
	Standard Name	uncertainty_dynamic_ocean_topography
	Definition	Uncertainty of the DOT measurements
Region Id	*Unit*	N/A
	Standard Name	region_code
	Definition	A regional mask for Arctic sea ice trends and climatologies
Instrument mode	*Unit*	N/A
	Standard Name	instrument_mode
	Definition	The mode that the SIRAL instrument was in at each measurement. Either LRM, SAR or SARin

2.2 Geographical Coverage

The Cryo-TEMPO Polar Ocean product covers the northern hemisphere, which is defined here as all CryoSat-2 SAR and SARin data north of 50°N (see Figure 2). Data in the southern hemisphere will be added in future versions.

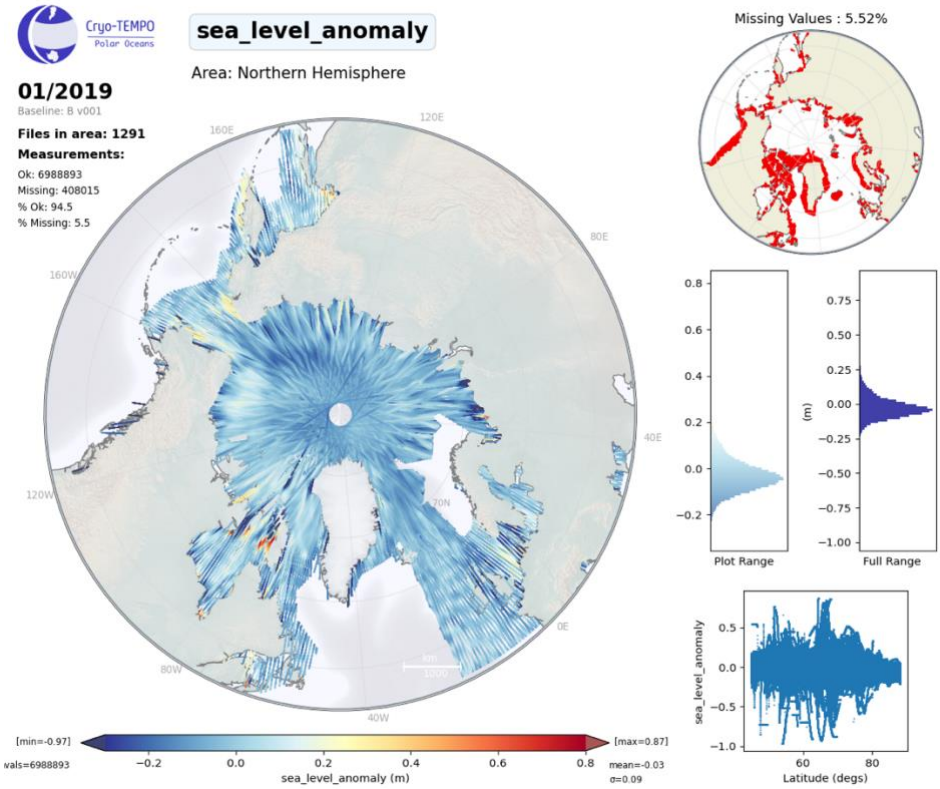

Figure 2. Geographical coverage of the Cryo-TEMPO thematic polar ocean product. This plot does not contain LRM open Ocean data, but will do so in the future.

2.3 Overall Processing Flow

The estimation of the along-track sea-level anomaly is processed with the SAMOSA+ retarcker (SAM+), which is incorporated into the PySiral work flow shared with the Sea Ice (SI) thematic product.

The fundamental principle of sea level anomaly and ocean dynamic topography retrievals are based on measuring the elevations of ocean surfaces from fractures in the ice cover. The open ocean measurements from CryoSat's LRM mode. Are calculated from the GOP L2 product. Sea level anomalies and ocean dynamic topography are then computed by taking the difference between the mean sea surface and the geoid, respectively, and the sea surface elevations along the ground track of the satellite (see Figure 1).

This processing chain is broken down into several distinct sub-steps (Figure 2):

1. Surface type classification of each waveform.

2. Estimation of radar range (retracking) for each waveform of the different surface types.

3. Application of range corrections due to varying radar wave propagation speed in the ionosphere and troposphere.

4. Removal of the effect of tides on the along-track elevations.

5. Along-track interpolation of the sea-level anomaly from the discrete observations of sea surface height in the ice cover.

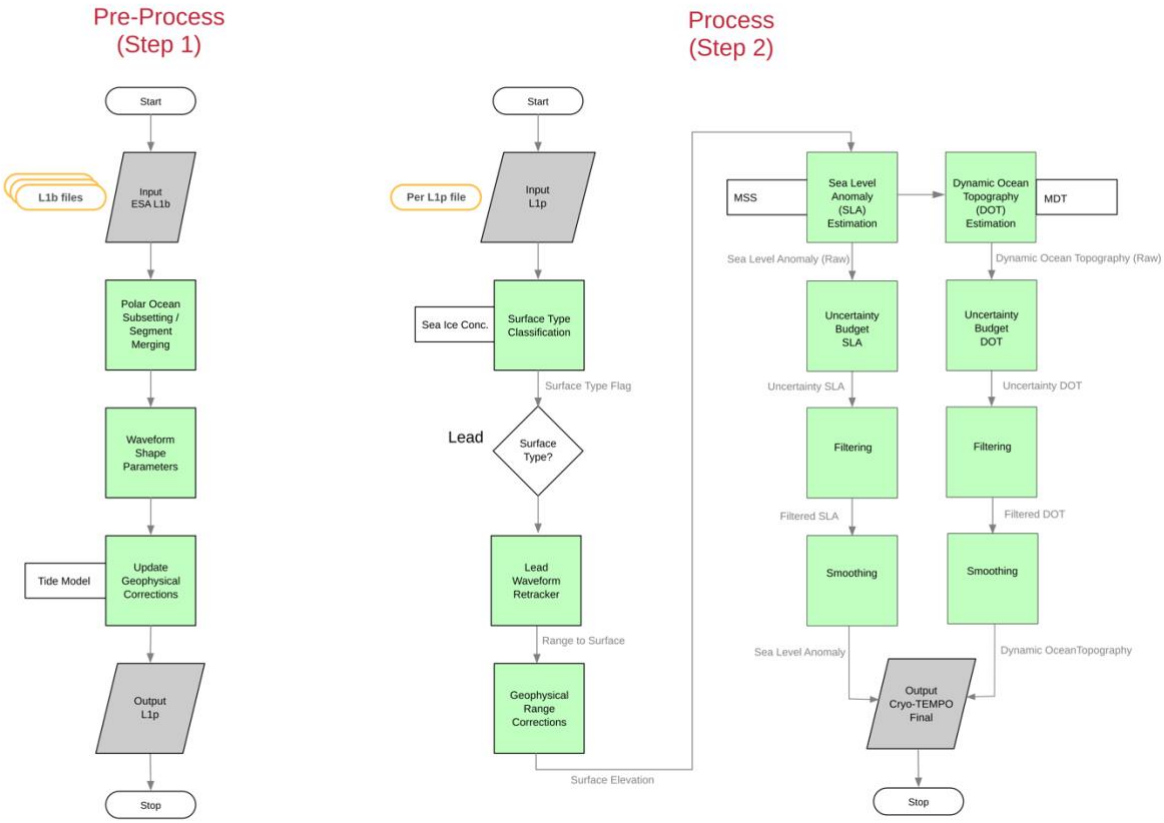

Figure 3. Processing workflow of geophysical retrieval of sea level anomaly (SLA) and dynamic ocean topography (DOT) for the Cryo-TEMPO Polar Ocean theme.

2.4 Source Data

Input data to the polar ocean processing algorithm falls into two categories:

1. Primary data: Radar altimeter data from the CryoSat's SIRAL.
2. Auxiliary data: External data sets aiding the calibration or geophysical retrieval.

Each data set is described in corresponding sections below.

2.4.1 CryoSat-2 altimeter data

Primary input data to the Cryo-TEMPO thematic polar ocean product is Level-1b data from the ESA CryoSat-2 baseline-D ICE processing chain for SAR and SARin radar modes [RD4]. The files are delivered as one netCDF file separated by changes of the radar mode. Information about the CryoSat-2 products of the ICE processor can be found here:

https://earth.esa.int/web/guest/missions/cryosat/ipf-baseline

The following variables are used from the baseline-D Level-1b netCDF files:

Table 2: List of variables from the CryoSat-2 level-1b primary input data for the polar ocean processing chain.

Time-orbit data	
time_20_ku	Data record time in TAI
lon_20_ku	Longitude of measurement
lat_20_ku	Latitude of measurement
alt_20_ku	Altitude of CoG above reference ellipsoid
SIRAL waveform data	
pwr_waveform_20_ku	Normalized echo power waveform
echo_scale_factor_20_ku	Echo Scale Factor (to scale echo to watts)
echo_scale_pwr_20_ku	Echo Scale Power (a power of 2)
window_del_20_ku	Window Delay (2way) corrected for instrument delays
Instrument Flags	
flag_mcd_20_ku	Level 1b Measurement Confidence Data
Flag	
surf_type_01	Surface type flag (1Hz, interpolated to time_20_ku)
region_id	Regional code (adapted from NSIDC region mask)
Range Corrections	
mod_dry_tropo_cor_01	Dry Tropospheric Correction (1Hz, interpolated to time_20_ku)
mod_wet_tropo_cor_01	Wet Tropospheric Correction (1Hz, interpolated to time_20_ku)
hf_fluct_total_cor_01	Dynamic Atmosphere Correction (1Hz, interpolated to time_20_ku)
iono_cor_01	Ionosphere Correction (1Hz, interpolated to time_20_ku)
solid_earth_tide_01	Solid Earth Tide Correction (1Hz, interpolated to time_20_ku)
pole_tide_01	Geocentric Pole Tide Correction (1Hz, interpolated to time_20_ku)

2.4.2 Auxiliary Data

Auxiliary data sets are data sets that are input to the geophysical retrieval but are not a measurement made by the CryoSat-2 radar altimeter itself. Auxiliary data sets can be static fields or data sets from satellite observations with variable temporal coverage and resolution.

2.4.2.1 Sea Ice Concentration

Daily sea-ice concentration fields at a spatial resolution of 25km are used as a sea ice mask in the sea-ice freeboard retrieval. The data source is the Global Sea Ice Concentration Climate Data Record produced by the European Organisation for the Exploitation of Meteorological Satellites (EUMETSAT) Ocean and Sea Ice Satellite Application Facility (OSI SAF).

The data is available in from a THREDDS Data Server (TDS) of MET Norway and through the Climate Data Store (CDS) of the Copernicus Climate Change Services (C3S).

Parameter	Sea ice concentration (sea ice area fraction)
Unit	percent
Data Source	MET Norway (https://thredds.met.no/thredds/c3s/c3s.html)
Data DOI	https://doi.org/10.24381/cds.3cd8b812

2.4.2.2 Mean Sea Surface Elevation

The global high resolution mean sea surface with a spatial resolution of 1 minute from DTU Space (Version DTU21) is used to facilitate the estimation of sea-level along the ground-track of CryoSat-2. This data set is static and used for the entire CryoSat-2 data record.

Parameter	Elevation of mean surface
Unit	meter
Data Source	DTU-SPACE (https://ftp.space.dtu.dk/pub/DTU21/1_MIN/)

2.4.2.3 Mean Dynamic Topography

The global high resolution Mean Dynamic Topography with a spatial resolution of 0.1250 degrees from DTU Space (Version DTU22) is derived from the XGM2019e geoid and DTU21 MSS used to facilitate the estimation of dynamic ocean topography along the ground-track of CryoSat-2. This data set is static and used for the entire CryoSat-2 data record. Similar to Knudsen et. al. (2019).

Parameter	Elevation of mean dynamic topography
Unit	meter

Data Source	DTU-SPACE

2.4.2.4 Uncertainty of the Mean Dynamic Topography

The global uncertainty field of the mean dynamic topography with a spatial resolution of 0.1250 degrees is sourced from DTU Space (Version DTU22). This data set is static and used for the entire CryoSat-2 data record (Knudsen et. al. 2019).

Parameter	Uncertainty of mean dynamic topography
Unit	meter
Data Source	DTU-SPACE

The technique applied to derive the MDT model makes it difficult to propagate the uncertainties analytically. In principle, the errors comprise of errors in the MSS and in the geoid model and short scale MDT signals that have been removed by the filtering process. The MDT error field is computed by a simple approach by deriving standard deviations associated with the weighted means of the MSS and the geoid given by:

$$\sigma_w^2 = \frac{\sum_{i=1}^{N} w_i \left(\Delta h_i - \overline{\Delta h}_w\right)^2}{\frac{N-1}{N}\sum_{i=1}^{N} w_i} \quad \text{where} \quad \overline{\Delta h}_w = \frac{\sum_{i=1}^{N} w_i \Delta h_i}{\sum_{i=1}^{N} w_i}$$

Where w_i is the weight of the i'th value coming from a filter and Δh_i is the MDT. The N values are located within a certain radius from the point of interest. The weighted mean heights $\overline{\Delta h_w}$ enter the MDT model. For more information see Knudsen et. Al (2019).

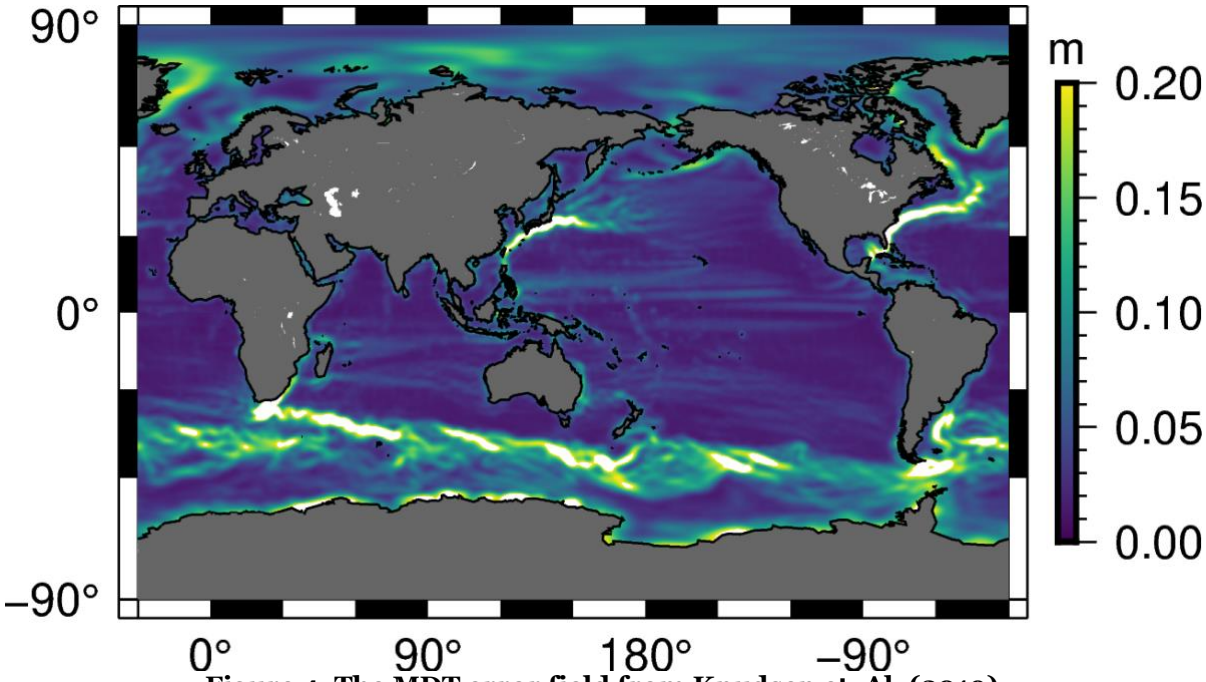

Figure 4. The MDT error field from Knudsen et. Al. (2019).

2.4.2.5 RegAT-Arctic regional tide

The RegAT-Arctic regional model (Cancet et al., 2022, in prep.) has been implemented in the framework of project funded by CNES and is an update of the Arctide2017 regional model (Cancet et al., 2018). Compared to the Arctide2017 model, the RegAT-Arctic atlas includes the Hudson Bay and the bathymetry has been improved in several regions around Greenland. In addition, a more recent and complete CryoSat-2 dataset was used to estimate tidal harmonic constituents and constrain the model with data assimilation. The RegAT-Arctic is composed of 34 tidal components, like the FES2014 global tidal model. The resolution of the RegAT-Arctic model mesh grid ranges between 2 km and 15 km along the coast, and up to 45 km in the deep ocean. We provide tidal elevations computed from the RegAT-Arctic regional model at each location and date of the CryoSat-2 measurements in the Arctic Ocean.

2.5 Sea Level Anomaly and Dynamic Ocean Topography

This section describes the sea level anomaly processing chain with input from all auxiliary data described in Section 2.4.2.

2.5.1 Pre-processing of Level-1b data

A regional subset of latitudes higher than 45 degrees in both hemispheres is used to limit the available CryoSat-2 L1b SAR and SARin data. For these two subsets, all data files from one orbit are merged into a single orbit segment, since input data may be distributed into different files based on the radar

mode. The objective is to create a continuous data segment over marine areas. Longer data segments over land are cropped from the data set (see Figure 5 for an example).

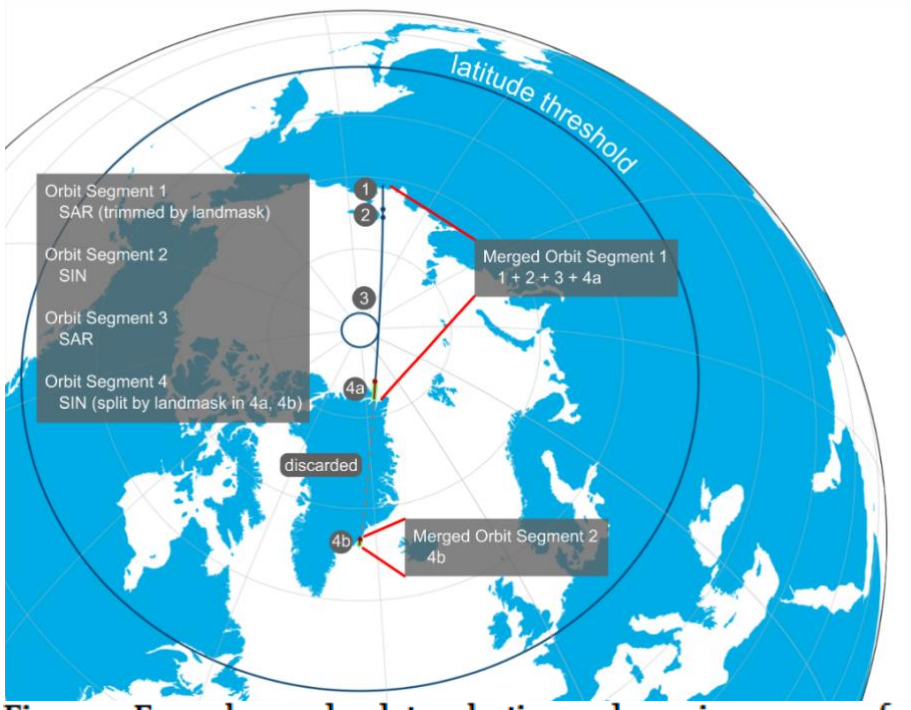

Figure 5: Exemplary radar data selection and merging process of SAR and SARin data

In addition, waveform shape parameters used for surface type classification (Section 2.6.2) are computed, the timestamp is converted from TAI to UTC and the merged L1b data subset is stored internally as a processing level 1-preprocessed (l1p) file on the production system.

2.5.2 Surface Type Classification

The first step in the sea level anomaly retrieval is the surface type classification for each waveform based on pre-computed waveform shape parameters. This work-flow is similar to the SI thematic product, but for the PO theme only the lead and open ocean observations are use. The objective is assigning each waveform one of the four classification values:

1. Open ocean: Measurement over water surfaces outside the sea ice cover.
2. Lead: Measurement over water surfaces inside the sea ice cover between sea ice floes or at sea ice fractures.
3. Ice Surface: Measurements that solely consist of sea ice surfaces.
4. Ambiguous: Measurements from mixed surfaces or where the classification has failed.

The surface type classification algorithm originates from algorithm development in the ESA Climate Change Initiative – Sea Ice Project (Paul et al., 2018) and classifies waveform based on three waveform parameters:

- Pulse Peakiness (PP)
- Leading Edge Width (LEW)
- Radar backscatter coefficient (SIGMA0)

The pulse peakiness PP is computed based on the power of each range bin WF_i, the maximum power of the waveform max(WF) and the number of range bins N_{WF} in the waveform:

$$PP = \sum_{i=1}^{N_{wf}} \frac{\max((WF))}{F_i} \cdot N_{WF}$$

The leading-edge width LEW is computed using the TFMRA retracker algorithm (see SI ATBD for power thresholds of 5 and 95%. The radar backscatter coefficient is computed after Dinardo, 2016.

The thresholds for the three parameters have independent values for SAR and SARin waveforms. In addition to the waveform-based classification, the sea-ice concentration data is providing the daily sea-ice mask and the land/sea flag (variable surf_type_01) from the L1b input data set is used to exclude any data over land. The latter is provided at 1Hz and is extended to all waveforms within the 0.1 second window. After classification, the surface type flag is merged with the land/sea flag for further use in the processor.

2.5.2.1 Open Ocean

Measurements over open ocean are classified solely by the sea-ice concentration auxiliary data set and the land/sea flag: Every waveform that is marked as ocean (variable surf_type_01 is 0) and where the sea ice concentration is below 70%. The threshold is higher than the usual value (15%) for the ice edge in sea-ice concentration data sets from passive microwave observations. The higher threshold is intended to prevent misclassifications of other surface types in loose ice conditions of the marginal ice zone and thus the open ocean domain intentionally includes potentially ice-covered region.

2.5.2.2 Lead Surface

Radar altimeter measurements over leads within the sea ice cover are characterized by specular reflection, resulting in narrow echoes with a high peak power. To be classified as a lead waveform, PP and SIGMA0 must exceed a minimum threshold, while LEW must be smaller than a maximum threshold.

The following parameter thresholds are valid for Arctic sea ice in the winter period between October and April:

Table 3: Waveform shape parameter thresholds for lead surface classification of CryoSat-2 SAR waveforms in the Arctic.

Arctic Leads (SAR)	SIC	PP		LEW		SIGMA-0	
	MIN	MIN	MAX	MIN	MAX	MIN	MAX
January	70%	69.90	-	-	0.76	23.40	-
February	70%	76.00	-	-	0.72	28.00	-
March	70%	73.80	-	-	0.73	25.80	-
April	70%	68.60	-	-	0.76	24.10	-
May	70%	69.90	-	-	0.76	24.10	-
June	70%	69.90	-	-	0.76	24.10	-
July	70%	69.90	-	-	0.76	24.10	-
August	70%	69.90	-	-	0.76	24.10	-
September	70%	69.90	-	-	0.76	24.10	-
October	70%	67.30	-	-	0.77	23.80	-
November	70%	66.30	-	-	0.78	23.20	-
December	70%	66.60	-	-	0.78	23.30	-

Table 4: Waveform shape parameter thresholds for lead surface classification of CryoSat-2 SARin waveforms in the Arctic.

Arctic Leads (SARin)	SIC	PP		LEW		SIGMA-0	
	MIN	MIN	MAX	MIN	MAX	MIN	MAX
January	70%	264.60	-	-	1.09	24.50	-
February	70%	291.80	-	-	1.02	29.00	-
March	70%	288.80	-	-	1.03	27.40	-
April	70%	272.60	-	-	1.07	25.80	-
May	70%	272.60	-	-	1.07	25.80	-
June	70%	272.60	-	-	1.07	25.80	-
July	70%	272.60	-	-	1.07	25.80	-
August	70%	272.60	-	-	1.07	25.80	-
September	70%	272.60	-	-	1.07	25.80	-
October	70%	264.30	-	-	1.10	24.90	-
November	70%	257.90	-	-	1.11	25.00	-
December	70%	253.60	-	-	1.13	24.10	-

2.5.2.3 Ambiguous Surfaces

All waveforms that are not classified as one of the other surface types or as land by the land/sea flag are designated as ambiguous.

2.5.2.4 Arctic Regions

The 2021 version of the regional mask for Arctic sea ice trends and climatologies defines commonly used regions relevant for Arctic sea ice as polygons for each region (Scott Stewart and Walter N. Meier,

NSIDC). The region definition was supplied by NSIDC in shapefile format and the id number of each region has been gridded on an EASE2 grid with a resolution of 1 km (Figure 4 and Table 4). The region id is added to each freeboard and snow depth value along the CryoSat-2 ground track to allow easy assessment of sea ice results by region.

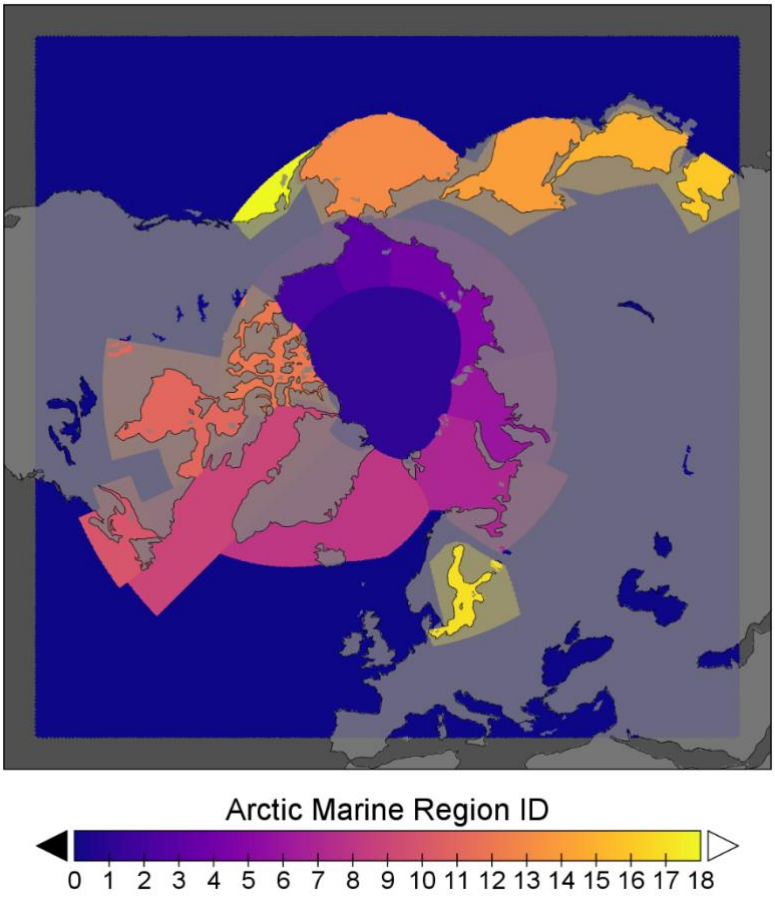

Figure 4: Map of region id's from the 2021 version of the regional mask for Arctic sea ice trends and climatologies (credit J. Scott Stewart and Walter N. Meier, NSIDC).

Table 4: Region id's and their name from the 2021 version of the regional mask for Arctic sea ice trends and climatologies (credit J. Scott Stewart and Walter N. Meier, NSIDC).

ID	Region Name	ID	Region Name
0	Undefined Region	10	Gulf of St. Lawrence
1	Central Arctic	11	Hudson Bay
2	Beaufort Sea	12	Canadian Archipelago
3	Chukchi Sea	13	Bering Sea
4	East Siberian Sea	14	Sea of Okhotsk

5	Laptev Sea	15	Sea of Japan
6	Kara Sea	16	Bohai Sea
7	Barents Sea	17	Baltic Sea
8	East Greenland Sea	18	Gulf of Alaska
9	Baffin Bay & Labrador Sea		

2.5.2.5 High resolution land mask

A gridded land-ocean mask for the Arctic regions at a resolution of 250 m has been created based on shapefiles of the OpenStreetMap[1] project except for the landmass of Greenland, which is sourced from the Natural Earth project[2]. The reason for the two-source solution is a better agreement of the Natural Earth shapefile with the Greenland topography from Global 30 Arc-Second Elevation (GTOPO30) digital elevation model, while the OpenStreetMap shapefiles provide more detail in the rest of the Arctic.

2.5.3 SAMOSA+ Retracker

The SAMOSA+ retracker is a “one-step” SAR Altimetry retracker based on the stack range integrated power (RIP) (Dinardo et al., 2021) In the frame of Cryo-TEMPO a special Python implementation of the SAMOSA+ retracker is developed from L1B. The main formulation of the code can be found in the ATBD for Coastal Ocean.

For the PO theme, the SAMOSA+ code deviates from the Coastal Ocean theme by several points. The Costal Ocean uses the GOP L1b data whereas the PO theme uses the GDR (ICE) L1b product.

- The Hamming Function is used in GDR (Ice), but not in the GOP product: set CONF.wf_weighted = True
- The stack zero-mask (as computed at L1b) is provided in the L1b products (this is not the case yet for GOP)
- For calculating Sigma0: We use the atmospheric attenuation as computed by the NOAA GFS model for the two ways atmospheric losses

The SAMOSA+ retracked Range is run separately and used as an input auxiliary file to the original TFMRA workflow (See SI ATBD). The auxiliary file will need to contain range and power estimates for each retracked location and a fill value for locations that were not retracked.

3 SURFACE ELEVATIONS AND RANGE CORRECTIONS

The range ***r*** and the altitude of the spacecraft $h_{spacecraft}$ provide information of the surface elevation $h_{surface}$ with respect to the reference ellipsoid. At this stage, the range has been computed based on vacuum light speed and corrections need to be applied for varying wave propagation speed depending on the condition of the troposphere and ionosphere. In addition, tidal corrections are applied to range for consistency of elevations of ocean surfaces for different data acquisitions:

$$hsurface = hspacecraft - r + \sum rc$$

The list of range corrections rc is the following:

- Ionosphere correction
- Dry troposphere correction
- Wet troposphere correction
- Dynamic Atmosphere correction
- Elastic ocean tide
- Long-period ocean tide
- Ocean loading tide
- Solid earth tide
- Geocentric polar tide
- Sea State Bias?

There are two data sources for the different range correction: Corrections for range effects caused by conditions in the ionosphere, troposphere as well as the inverse barometric effect and the solid earth tide and polar tide are based on information present in the Level-1b primary input data (see section 2.5.1). The remaining tidal corrections are sourced from the more recent and improved FES (Finite Element Solution) global tide model that has been developed by a consortium with LEGOS, Noveltis, CNES and CLS as members.

The sea level derived from the SAMOSA+ retracker is also corrected for sea state bias. The sea state bias is a range error due to the ocean waves. In leads in the sea-ice cover the SSB is very close to zero. It is a combination of the electromagnetic bias, the skewness bias, and the tracker bias. The electromagnetic bias arises from the unequal surface scattering affecting the radar return. The mean scattering is shifted from nadir due to the fact that wave troughs are better reflectors than wave crests. This shift tends to overestimate the range. The skewness bias is related to the faulty assumption of the onboard tracker symmetry. The tracker bias is an instrument error linked to tracking ocean echoes.

The Cryo-TEMPO SSB is derived from a bilinear interpolation table of sea state bias versus significant wave height (SWH) and the wind speed. The table is estimated from an empirical fit (Labroue et al., 2004) The SWH and wind speed is estimated from the SAMOSA+ retracker.

From the GOPM product the following variables are used to derive the SLA:

SLA = GOP[ssha] + GOP[MSS] + GOP[ocean_tide]- GOP[load_tide] - GOP[SSB] - tides- MSS

Where the origin of the variables are shown below.

Name	GOP[ssha]	GOP[MSS]	GOP[ocean_tide]	GOP[load_tide]	GOP[SSB]	tides	MSS
Origin	GOPM	GOPM	GOPM	GOPM	GOPM	LEGOS/Noveltis/CNES/CLS	DTU
Product Name	ssha_20_ku	Mean_sea_surface_sol1_01	Ocean_tide_sol1_01	Load_tide_sol2_01	Sea_state_bias_01_ku	FES2014b/ RegAT-Arctic	DTU21

Sea Surface Anomaly and Dynamic Ocean topography

After application of the range correction, the surface heights are split into two categories, the heights of lead surfaces and the heights of sea ice surfaces. In the Polar Ocean Product, the sea ice is discarded and set to not-a-number.

The heights of the lead surfaces with respect to the mean sea surface (MSS) yield raw observations of the sea level anomaly (sla_{raw}) at discrete locations where the surface type classification indicates the presence of a lead:

$$sla_{raw} = h_{surface}\,[surface\,type \equiv lead] - mss$$

The sla_{raw} is then interpolated and smoothed, providing a continuous sea level anomaly (sla):

$$sla = func(sla_{raw})$$

This function contains several main processing steps:

1. Smooth sla_{raw} with a box filter with filter size of 100km to reduce the raw noise of the observations. This step is only applied to the existing observations. The filter size width has

been chosen empirically as a compromise between reducing noise and retaining true spatial variability of the sea surface height.

2. Apply a linear interpolation between the smoothed raw sea-level anomaly observations for the entire trajectory.

3. Apply a box-filter smoother to the interpolated values with the same filter size as before (100 km).

4. Set the result to NaN (not a number) if the closest $slaraw$ observation is not within two times the filter size (200km).The output is a smoothed and interpolated sea-level anomaly (sla) that extends along the entire ice-covered area if enough leads are present.

The uncertainty of this approach is parametrized with the following formular and based on the distance d_{tp} to the next sla_{raw} tie point. The uncertainty increases with distance to raw sea-level anomaly observations and reaches its maximum at 100km. The uncertainty reaches its minimum at the location of a raw sea-level anomaly observation and it is assumed that the smoothing process results in an uncertainty of 0.02 m:

$$\sigma_{SLA} = \begin{cases} 0.02m + 0.1m \times \left(d_{tp\,/\,100km}\right)^2, & d_{tp} < 100\ km \\ 0.1m\,, & d_{tp} \geqq 100\ km \end{cases}$$

with the assumption that the mean sea surface uncertainty is included in the sea level anomaly uncertainty.

The DOT is the sea level height above the geoid, and can be expressed by:

$$DOT = SLA + MDT$$

The DOT uncertainty is given by:

$$\sigma^2{}_{DOT} = \sigma^2{}_{SLA} + \sigma^2{}_{MDT}$$

where $\sigma^2{}_{MDT}$ is the uncertainty given by the MDT error field described in Section 2.4.2.4.

3.1.1 Filtering

As a final step in the processing, the sea level anomaly and the dynamic ocean topography outliers are removed and set to not-a-number (NaN) to exclude unrealistic observations likely due to a misclassification or surface targets that are not ocean, e.g., sea ice.

4 ASSUMPTIONS AND KNOWN ISSUES

There are several known limitations and error contributions in the Polar Ocean sea level retrieval process with radar altimeter data, which affects the uncertainty of the variables in the Cryo-TEMPO thematic polar ocean product.

1. The final SLA and DOT products are interpolated over great distances. There is a possibility of interpolating false values. This is especially the case when the satellite moves from the open ocean to the ice cover, while the marginal ice zone is the most rigorous area for the Polar Ocean processing.
2. The SARIn data is processed through SAM+ and the position is not corrected, and is therefore processed as SAR.

5 REFERENCES

Andersen, O. B., Abulaitijiang, A., Zhang, S., and Rose, S. K.: A new high resolution Mean Sea Surface (DTU21MSS) for improved sea level monitoring, EGU General Assembly 2021, online, 19–30 Apr 2021, EGU21-16084, https://doi.org/10.5194/egusphere-egu21-16084, 2021.

Cancet, M., Andersen, O., Lyard, F., Cotton, D., and Benveniste, J.: Arctide2017, a high-resolution regional tidal model in the Arctic Ocean, Advances in Space Research, Vol. 62, No. 6, p. 1324-1343, https://doi.org/10.1016/j.asr.2018.01.007https://doi.org/10.1016/j.asr.2018.01.007, 2018

Cancet, M., Lyard F., Toublanc F., Pineau-Guillou L., Sahuc E., Fouchet E., Dibarboure G., Picot N., The RegAt high-resolution regional tidal model in the North-East Atlantic Ocean: implementation and examples of applications, in preparation (2022)

Khvorostovsky, K.; Hendricks, S.; Rinne, E. Surface Properties Linked to Retrieval Uncertainty of Satellite Sea-Ice Thickness with Upward-Looking Sonar Measurements. Remote Sens. 2020, 12, 3094. https://doi.org/10.3390/rs12183094

Labroue, S., P. Gaspar, J. Dorandeu, O. Z. Zanifé, F. Mertz, P. Vincent, and D. Choquet, 2004: Nonparametric estimates of the sea state bias for the Jason-1 radar altimeter. Mar. Geod., 27, 453–481

Lavergne, T., Kern, S., Aaboe, S., Derby, L., Dybkjaer, G., Garric, G., Heil, P., Hendricks, S., Holfort, J., Howell, S., Key, J., Lieser, J. L., Maksym, T., Maslowski, W., Meier, W., Muñoz-Sabater, J., Nicolas, J., Özsoy, B., Rabe, B., Rack, W., Raphael, M., de Rosnay, P., Smolyanitsky, V., Tietsche, S., Ukita, J., Vichi, M., Wagner, P., Willmes, S., & Zhao, X. (2022). A New Structure for the Sea Ice Essential Climate Variables of the Global Climate Observing System, Bulletin of the American Meteorological Society, 103(6), E1502-E1521.

Markus, T. and Cavalieri, D.J. (1998). Snow Depth Distribution Over Sea Ice in the Southern Ocean from Satellite Passive Microwave Data. In Antarctic Sea Ice: Physical Processes, Interactions and Variability, M.O. Jeffries (Ed.). https://doi.org/10.1029/AR074p0019

Paul, S., Hendricks, S., Ricker, R., Kern, S., and Rinne, E.: Empirical parametrization of Envisat freeboard retrieval of Arctic and Antarctic sea ice based on CryoSat-2: progress in the ESA Climate Change Initiative, The Cryosphere, 12, 2437–2460, https://doi.org/10.5194/tc-12-2437-2018, 2018.

Ricker, R., Hendricks, S., Helm, V., Skourup, H., and Davidson, M.: Sensitivity of CryoSat-2 Arctic sea-ice freeboard and thickness on radar-waveform interpretation, The Cryosphere, 8, 1607–1622, https://doi.org/10.5194/tc-8-1607-2014, 2014.

Rostosky, P., Spreen, G., Farrell, S. L., Frost, T., Heygster, G., & Melsheimer, C. (2018). Snow depth retrieval on Arctic sea ice from passive microwave radiometers—Improvements and extensions to multiyear ice using lower frequencies. Journal of Geophysical Research: Oceans, 123, 7120– 7138. https://doi.org/10.1029/2018JC014028

Warren, S. G., Rigor, I. G., Untersteiner, N., Radionov, V. F., Bryazgin, N. N., Aleksandrov, Y. I., & Colony, R. (1999). Snow Depth on Arctic Sea Ice, Journal of Climate, 12(6), 1814-1829. Retrieved Feb 17, 2021, from https://journals.ametsoc.org/view/journals/clim/12/6/1520-0442_1999_012_1814_sdoasi_2.0.co_2.xml

Knudsen, P., Andersen, O., & Maximenko, N. (2019). A new ocean mean dynamic topography model, derived from a combination of gravity, altimetry and drifter velocity data. *Advances in Space Research*, 1–13. https://doi.org/10.1016/j.asr.2019.12.001

Salvatore Dinardo, Luciana Fenoglio-Marc, Matthias Becker, Remko Scharroo, M. Joana Fernandes, Joanna Staneva, Sebastian Grayek, Jérôme Benveniste, A RIP-based SAR retracker and its application in North East Atlantic with Sentinel-3, Advances in Space Research, Volume 68, Issue 2, 2021, Pages 892-929, ISSN 0273-1177, https://doi.org/10.1016/j.asr.2020.06.004.